

Chlorosulphonated Polyethylene and Its Composites for Electronic Applications

Sayan Ganguly and Narayan Chandra Das

Abstract Chlorosulphonated polyethylene (CSM) occupies an emerging field due to its immense flexibility, excellent heat resistance, excellent oil resistance as well as water resistance, good flame resistance and weathering resistance, and desirable compression set. Generally, this rubber contains 27–45 % chlorine and very nominal sulphur content (approximately 0.8–2.2 %). The enormous improvement in physical, mechanical, and dielectric properties as well as electrical and thermal conductivity of the entire CSM rubber composites is due to the addition of the particulate fillers including conductive fillers. The physico-mechanical behaviour of the composites is quite captivating with respect to other rubber composites in a wide temperature range viz. -80 to 160 °C. It can be used in low-voltage applications in cables where dielectric strength is 500 V/mil with dielectric constant 8^{-10} at 1000 Hz and dissipation factor in the range of 0.05–0.07 at 1000 Hz. CSM is widely practiced in exteriors or outer protective jackets in high-voltage applications due to its outstanding weather-resistant property. Meanwhile, CSM is also widely applied in the fabrication of composites to minimize the effect of radiation pollution emitting uncontrollably from electronic devices. CSM can uptake desirable amount of conducting filler for enrichment or improvement of the conductivity solely to the composites. It is not a hard and fast rule to make the composite highly conducting to inhibit radiation. It is required a conducting pathway to make the composite conducting that can interact with the electromagnetic wave and reduce its adverse effect. Here, the basic three types of mechanisms of radiation shielding are elucidated to culminate the development of CSM rubber-based electromagnetic interference (EMI)/radiation shielding materials with sufficient flexibility, weather resistance, and chemical resistance features.

S. Ganguly · N.C. Das (✉)

Rubber Technology Center, Indian Institute of Technology, Kharagpur 721302, India
e-mail: ncdas37@gmail.com; ncdas@binghamton.edu

Keywords Chlorosulphonated polyethylene • Conducting filler • Dielectric property • Conductivity • Protective jackets • Electromagnetic interference shielding

Abbreviations

CSM	Chlorosulphonated polyethylene
EMI	Electromagnetic interference
NR	Natural rubber
ASTM	American Society for Testing and Materials
EVA	Ethylene-vinyl acetate
EPR	Ethylene propylene rubber
NBR	Acrylonitrile butadiene rubber
ENR	Epoxidized natural rubber
PE	Polyethylene
LLDPE	Linear low-density polyethylene
HPC	Hydroxypropyl cellulose
AIBN	Azoisobutyronitrile
SBS	Styrene–butadiene–styrene
SNR	Sulphonated natural rubber
C_B	Bulk capacitance
R_B	Bulk resistance
PANI	Polyaniline
CNTs	Carbon nanotubes
SWCNT	Single-wall carbon nanotube
IDE	Interdigitized electrode
HCPE	High chlorinated polyethylene
TEM	Transmission electron microscope
RL	Reflection loss
UV	Ultraviolet
NPPs	Nuclear power plants
EAB	Elongation at break
BACN	Bromoacenaphthylene
MEM	Microelectromechanical
THF	Tetrahydrofuran
NaSS	Sodium 4-styrenesulphonate
HNBR	Hydrogenated nitrile butadiene rubber
U_e	Strain energy density
SE	Shielding effectiveness
dB	Decibel
RFI	Radio-frequency interference
ESD	Electrostatic discharge

IC	Integrated circuit
DBSA	Dodecyl benzene sulphuric acid
CSA	Camphor sulphonic acid

1 Introduction

Chlorosulphonated polyethylene abbreviated as CSM (as per ASTM D1418 rule) is an elastomeric material. The trade names of CSM are KhSPE in the USSR and Hypalon in the USA. CSM is a product of the chemical modification of polyethylene (PE), having a density of 1.11–1.26 g/cm³, which can be prepared from free radical triggered reaction (low density) of linear PE. CSM is insoluble in aliphatic hydrocarbon and alcohol, slightly soluble in ketones and esters, and readily soluble in aromatic hydrocarbons, such as toluene and xylene, and in chlorinated hydrocarbon. Chlorine content ranges generally from 24 to 43 %, and it is also reported that chlorine content is almost 30 % in case of branched Hypalon 20 and 35 % for linear Hypalon 40. The ability of Hypalon to retain its electrical property after long-term exposure to heat and water is spectacular. These properties make it a commercially viable insulation material in cable sheath compound ingredient in low-voltage applications, particularly in power cable (up to 600 V), control cable, mine trailing cable, locomotive cables, nuclear power station cable, automotive purpose cable, and so on. It is also drawing attention due to easy colourability and unfading after a prolonged time of exposure in atmosphere. It has an important intrinsic property of ozone resistance. There will be no sacrificial lagging due to its colourant incorporation also. Due to almost 30 % halogen content, it is self-extinguishing which leads it to a potential commercially applicable flame-resistant flexible cable coating. The abrasion resistance is superior to natural rubber (NR) and many several elastomers. High flexibility of this rubber in compounded form also marketed this in a dynamic application-related service. The effective chlorine content in the CSM prohibited the termite as well as micro-organism attack towards it, and that is why there will be no such mould growth, mildew, fungus, or bacterial are observed. The extensive wide range of temperature tolerance is another aspect of this material to maintain its position in the commercial sector. The flexibility is also sustained at –40 °C which makes this material a low-temperature applicable material with desired flexibility [1]. Physical and mechanical properties of CSM are summarized in Table 1. Owing to versatility properties, CSM is used for automotive hoses, gas and industrial applications, electric cable jacketing, machine parts, floor tiles, magnetic rubber, rubber-coated cloth, coatings, gaskets, flexible tubes, rolls and linings, and EMI shielding. Special applications for CSM can include escalator handrails, diaphragms and lining for chemical processing equipment, sensors, and actuator. Now a day Hypalon trademark has become a common name for all kind of CSM regardless of manufacturer, for example, Halion CSM from Lianda (distributed by Alternative Rubber & Plastics) and TOSO-CSM® and extos® alkylated chlorosulphonated polyethylene from

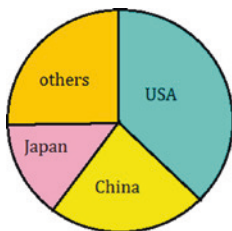
Table 1 Physical and mechanical properties of CSM (Hypalon)

Specific gravity	1.08–1.28
Brittle point (°C)	–40 to –62
Dielectric strength (V/mil)	500
Dielectric constant @ 1000 Hz	$8-10$
Dissipation factor @ 1000 Hz	0.05–0.07
Tensile strength (MPa)	17.236
Elongation (% EB)	430–540
Hardness (shore A)	60
Abrasion resistance	Excellent
Continuous use temperature (CUT)	121 °C
Impact resistance	Good
Compression set (%)	
@ 70 °C	25
@ 100 °C	44
@ 121 °C	16
Diffused sunlight resistance	Excellent
Effect of ageing	None
Heat resistance	good

TOSOH of Japan and a variety of CSM products from Jiangxi Hongrun Chemical Co., Ltd.

Versatile types of conducting filler are developed to enhance the electrical behaviours of CSM. The most common filler practiced was polyaniline (PANI)-based materials for their cost-effectiveness as well as for their easy production, improved thermal stability, and suitable dispersion in the rubber matrix. The present scenario in the total world market in the production of CSM rubber according to the economic report is pictured (Fig. 1).

The USA, China, and Japan showed nearly 80 % of the world consumption of CSM elastomers in 2011 and expected to grow of annual world consumption approximately 1.7–1.8 % during 2011–2017.

**Fig. 1** World consumption of chlorosulphonated polyethylene (2011)

2 Why Chlorosulphonated Polyethylene?

Hypalon is the registered trademark for a series of CSM developed by DuPont Dow Elastomers, USA. Besides several elastomers, CSM engrosses a significant area of elastomer blending. This amorphous, vulcanizable elastomer (Dupont, UK) was formerly applied as solution coating applications. The basic structure of CSM rubber is shown in Fig. 2. The value of z shown in Fig. 2 is usually 17, the typical value of $(x + y)$ is 12 and $z > (x + y)$. There various grades which serve the electrical application fields are jotted down (Table 2) [2].

Generally, when NR is blended with CSM, there is an observation that oil, ozone/oxygen, heat resistance, and elastomers can be improved in a greater degree. It is customary to say that the blend behaviour is potentially dependent on the CSM to other elastomer ratio in the composite blend. Improved oil and thermal ageing resistance were observed when other elastomers were blended with chlorinated polyethylene (CPE). That is why it is used as protective coating or sheath compound materials in cable jacket. Before an era, blends of CSM with NR have been studied by Tanrattanakul and Petchkaew at 2006 [3]. Several elastomer blends are already studied based on CSM due to its potential stability against thermal atmosphere and sunlight. There are a couple of publications that have discussed rubber blends based on CSM, including CSM/EVA [4–6], CSM/EPR [7, 8],

Fig. 2 Structure of chlorosulphonated polyethylene

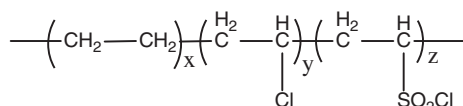


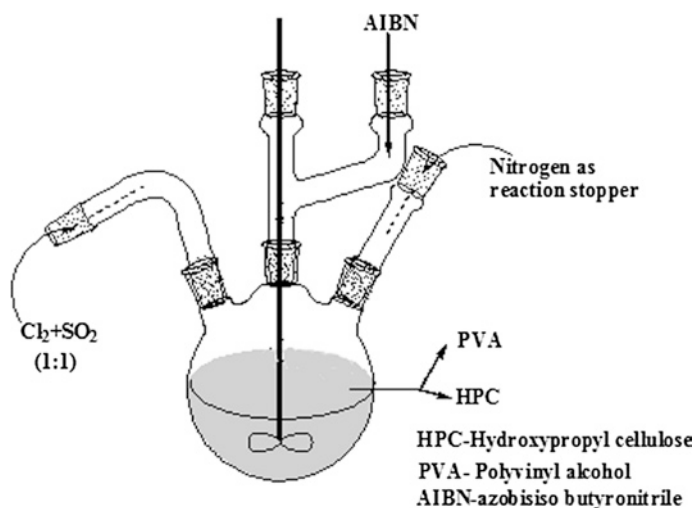
Table 2 Available grades according to their applications [2]. Copyright 1982. Reproduced with permission from John Wiley & Sons

Quality parameters	Grades							
	20	30	40 soft	40	4085	45	48 soft	48
Chlorine content (%)	29	43	35	35	35	25	43	43
Sulphur content (%)	1.4	1.1	1.0	1.0	1.0	1.0	1.0	1.0
Sp. Gravity	1.14	1.26	1.18	1.18	1.18	1.07	1.27	1.27
Mooney at 100 °C	30	30	45	55	85	40	62	77
Applications	Primary solution coating		General purpose, extruded, calendered, moulded, coloured and black			Hard vulcanizates with moderate loading		Extruded, calendered, and moulded goods with superior oil resistance
						Unvulcanized compounds with good physical properties		

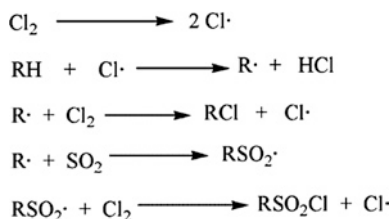
CSM/NBR [9–12], and CSM/ENR [11–13]. Another aspect for choosing this CSM is that its curing can be tuned inherently in the blend as reported elsewhere, so it is named as “self-vulcanizable rubber blends” [11, 14–17].

2.1 Synthesis Methods of Chlorosulphonated Polyethylene

CSM is synthesized by either solution method, or gas–solid method, or aqueous solution-suspension method. At present, DuPont Dow Elastomers and Jilin petrochemical company produced CSM via solution method in CCl_4 solvent. But the recurring problem for using CCl_4 is its ozone depleting behaviours just like other halo methanes viz. Freons types. There is no other reasonable alteration of CCl_4 solvent to prepare CSM by solution method in the literature. Hence, it is accepted that development in synthetic strategy of CSM is decelerating. Therefore, the development of CSM becomes slow. There are several patents available on preparation of CSM by gas–solid method using PE and a gaseous mixture of chlorine and sulphur dioxide. As an emerging engineering polymeric material, the performance of CSM nearly related to their internal architecture, particularly crystallization process during the production and processing of CSM. In order to enhance the desirable properties of end products, the optimization conditions are adjusted for an industrial process. Wang et al. confronted an aqueous solution-suspension method where a sulphur and chlorine incorporation in LLDPE backbone by means of permutations was done [18]. A typical synthesis scheme of CSM in the aqueous solution-suspension method is shown in Scheme 1.



Scheme 1 Synthesis scheme of CSM in aqueous solution-suspension method



Scheme 2 Proposed mechanistic pathway for the solution-suspension method

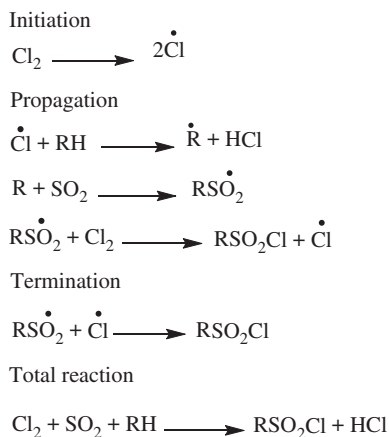
The aqueous solution-suspension method for CSM preparation is depicted in Scheme 2.

In this work, the CSM with several contents of chlorine and sulphur elements was successfully prepared by an aqueous solution-suspension method. The productive introduction of $-\text{Cl}$ and $-\text{SO}_2\text{Cl}$ groups to the polymers was confirmed by FTIR spectra and also by ion chromatography [18].

Another almost recent method for synthesizing CSM is gas–solid method. The gas–solid method is a novel fashion to prepare CSM compared to the conventional solution procedure which is inexpensive and green process in terms of environment pollution in the absence of solvent. Many patents are available on synthesis of CSM through the gas–solid method using PE and a gaseous mixture of chlorine and sulphur dioxide [19, 21, 22].

Chlorosulphonation of PE by the gas–solid method is not a trouble-free operation. As a highly crystalline feed material, like PE it is very unfortunate to initialize chlorosulphonation reaction under melting temperature of PE. Such type of chlorosulphonation temperature will lead to the aggregation of PE particles, which may forbid the progress of reaction. Noeske et al. discovered a process for chlorosulphonation of PE in a fluidized bed within a temperature range of 40–80 °C [19]. The chlorosulphonated end product prepared with this fluidized bed method is typically not amorphous materials due to sufficient residual inherent crystalline domains already in the feed PE. Later, CSM is also synthesized by the gas–solid method in a tank reactor using CPE and a gaseous mixture of chlorine and dioxide sulphur within a temperature range of 30–50 °C [20]. Another modernized method involves the reaction of amorphous CPE with a gaseous feed mixture of chlorine and sulphur dioxide in a fluidized bed. The yield or the transformation to CSM is much better than using crystalline PE as feed because amorphous nature of CPE. When the crystallinity of amorphous CPE is >15 wt%, and chlorination does not occur in chlorosulphonation, so the reaction can be fulfilled at lower temperature than utilizing PE [23]. The reaction was implemented at a temperature range of 25–100 °C, for a period of more or less 2 h. This process is more acceptable than using crystalline PE as the starting material, but the reaction has not been comprehensively studied. The chemical equation of the chlorosulphonation of CPE is a free radical chain mechanism as shown in Scheme 3.

Scheme 3 Preparation of CSM in gas–solid method



3 Filler-Impregnated Chlorosulphonated Polyethylene Composites

A wide range of CSM grades have been used for wire and cable insulation. Older materials include NR, butyl rubber, and styrene–butadiene rubbers (SBR). Younger material community includes crosslinked PE, silicone rubber, ethylene–propylene elastomers, modified or chlorosulphonated polyethylene, and thermoplastic elastomers to overcome the ageing possibility of the compounds. Properties of grandness to electrical insulation exponent include dielectric constant, resistivity, dielectric loss, and dielectric strength. Flame resistance is also important in certain applications.

Sulphonated ionomer moiety in a polymeric material, bearing with a hydrophobic organic backbone chain and a comparatively modest amount of pendant ionic sulphonate groups ($-\text{SO}_3^-$) counterbalanced by metal counter ions. A concern in sulphonated ionomer (here CSM) is primarily due to its unique properties, derived from strong associative interactions between ionic groups [24]. In another experiment, the formulation of a quaternary ammonium ionomer of styrene–butadiene–styrene triblock copolymer (SBS) was modernized by a ring opening reaction of epoxidized SBS with triethylamine hydrochloride in the presence of phase transfer catalyst and later on blended with CSM rubber. Thus, the oil-resistant character as well as its electrical application is attributed [25]. Boonsong et al. hypothesized a novel rubbery ionomer of zinc salt of sulphonated NRs (Zn-SNR) and used it as an eminent compatibilizer for the blends of NR and CSM. Establishment of these blending techniques enhances the electrical applicability of CSM rubbers, and in addition, this makes the place in commercialize field [26]. Conductive carbon black (CB) incorporation into the rubber matrix is an effective and easy pathway to make conducting composite for shielding applications. Here, Ensaco 350G, a conducting black, was used in CSM matrix to enhance the conducting property

without parting the conductive quality of that composite; 30 phr loading of Ensaco 350G achieves better results without any agglomeration [26]. In this paper, the author revealed that the effect of filler loading is a function of real part of impedance. The complex impedance will be in Eq. 1;

$$Z^* = Z' + jZ'' \quad (1)$$

where Z' and Z'' are real and imaginary parts, respectively. Z' interprets the resistive part of the system and Z'' renders the reactance arising due to the capacitive or inductive nature of the system. Regardless of the filler loading, there is a gradual drop-off of real impedance with increase in frequency, and at higher frequencies (105–106 Hz), the effect is in borderline (Fig. 3). Relaxation phenomenon in crosslinked and reinforced polymer assemblies is basically a hinge on the chemical and physical interactions between the viscoelastic polymer phase and solid filler phase. Crosslinking of the polymers unremarkably enforces intermolecular restraints, which in turn play a crucial role in the segmental dynamics of all polymeric arrangements in the bulk state [27]. Incorporation of fillers such as conductive CB (here used Ensaco 350G) not only results in hydrodynamic interactions but also leads to complex physicochemical interactions between the polymer matrix and the filler surface [26].

Nanda et al. hypothesized another study for the effective filler loading which was supported by Nyquist plots [28]. According to Sluyters-Rehbach and Sluyters, the total impedance of the cell is the series of combinations of resistors, R_B , and capacitors, C_B . Especially in a Nyquist plot of polymer composite system (Fig. 4), the real part of impedance in real axis interprets bulk resistance (R_B) and imaginary axis represents ω_{\max} (viz., top of the semicircle) and is given by Eq. 2 [26];

$$\omega_{\max} = \frac{1}{R_B C_B} \quad (2)$$

where C_B is bulk capacitance of the polymer composite.

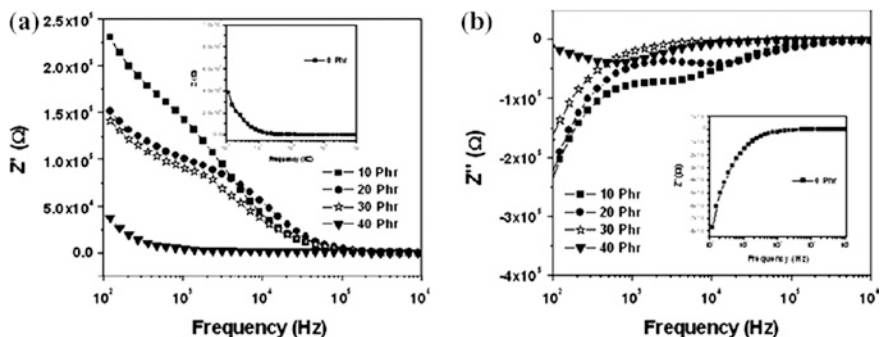
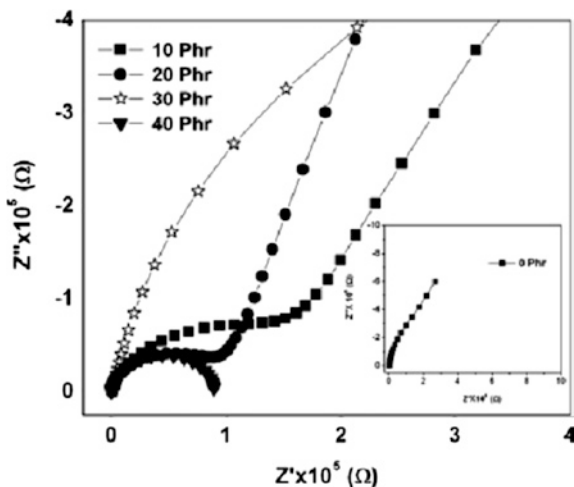


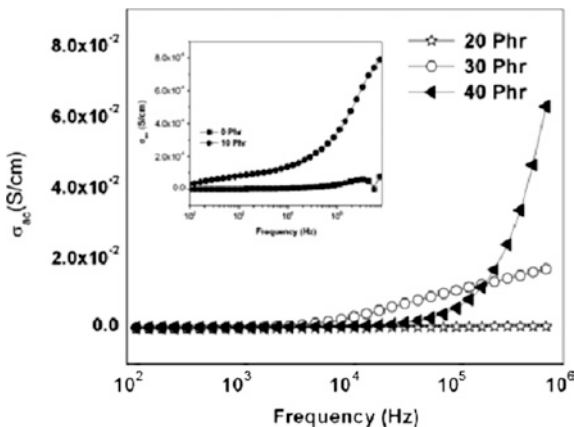
Fig. 3 Effect of filler loading on (a) real part of impedance (Z') and (b) imaginary part of impedance (Z'') of CSM vulcanizates as a function of frequency at 30 °C [26]. Copyright 2012. Reproduced with permission from John Wiley & Sons

Fig. 4 Nyquist plot (Z'' vs. Z') for different filler loadings in CSM vulcanizates at 30 °C [26]. Copyright 2012. Reproduced with permission from John Wiley & Sons



With increase in filler loading, there is a decrease in R_B , which represents increase in conductivity and less lossy response. However, with increase in filler loading, there is a gradual improvement in bulk capacitance (C_B). The gaps in the plot between the C_B aggregates control the electron conduction via non-Ohmic pathway contacts between the C_B agglomerates. The cores of the semicircle plot and the bulk resistance (R_B) values for all experimented filler loading have been elucidated in the plot. The shift in the centre of the semicircle can be used as an evaluation of the breaches in between the agglomerated islands of C_B particulates. It was also discovered that with increase in filler loading, the R_B value is decreasing and core of the semicircle is also decreasing. This may be due to enhancement in conductivity with increase in filler loading, which agreed well with the conductivity plot given in Fig. 5.

Fig. 5 Variation in ac conductivity (σ_{ac}) with frequency for different filler loadings in CSM vulcanizates at 30 °C [26]. Copyright 2012. reproduced with permission from John Wiley & Sons



In recent researches, the hybrid fillers act as potential conducting phase in any rubber matrices. Here the main focus is on CSM rubbers where a novel carbonyl iron powder and graphite was used to make more productive conducting composites [29]. The dual behaviour of the composite viz. electric and magnetic sensitivity was also noticed in these types of composites. Such composite absorbent has the maximum magnetic loss for electromagnetic wave at 12.82 GHz and can affect high dielectric loss on the high frequency; hence, this type of composites may serve as a potential shielding material. Marković et al. [30] had considered the effect of gamma radiation on the degradation of blends of NR and CSM [31]. From that standpoint, the CSM-related areas are nurtured by gamma treatment. The effect of gamma irradiation on the acrylonitrile butadiene/chlorosulphonated polyethylene rubber blend (NBR/CSM)-based nanocomposites carrying C_B and silica filler was investigated by Marković et al. also. These nanocomposites containing 20 phr of silica and 30 phr of C_B , respectively, showed high polymer–filler interaction and low filler–filler interaction, so suitable properties are achieved which can drive these CSM-based composites into electrically applicable. Synergism is a predominant effect while 20 phr of silica and 30 phr of conducting C_B -filled NBR/CSM nanocomposites amended the thermal stability, mechanical properties, and conductivity [32].

Emulsion polymerization technique is another process to develop composites. CSM rubber can be enriched with conducting property by incorporation of conducting polymeric fillers with enhanced phase adhesion property. Polymerizing aniline in the presence of CSM rubber where conducting PANI is dispersed phase and CSM rubber solution acts as dispersing medium. The main attraction in this method is that it is low-temperature fabrication technique where thin coherency is maintained. Besides, this conducting sulphur-bearing CSM is used here. Consequently, the composite exposed a discharge capacity of 117.3 mAhg^{-1} and the capacity retention remained at about 78 % after twenty-two cycles, based on the second cycle discharge capacity. Here, PANI officiated as both electrocatalyst and cathode material. At the same time, it improved the conductivity of the active CSM at a molecular level. The results of this study provided a new thought for structure design and development of a potential cathode material for rechargeable magnesium batteries [33]. Among the several nanomaterials, carbon nanotubes (CNTs) have experienced substantial attention due to their unique electronic and extraordinary mechanical properties associated with electrical conductivity [34]. Single-wall carbon nanotubes (SWCNTs) have also a tremendous surface area, as high as approximately $1600 \text{ m}^2/\text{g}$ [35]. A chemical sensor is fabricated using the CSM rubber nanocomposite where CNT plays a important role in order to construct the mechanically strong as well as electrically potential nanocomposite. He fabricated a simple sensor platform comprising of an interdigitized electrode (IDE) pattern for sensing gas and organic vapours. Purified SWCNTs in the form of a network bedded on the IDE by solution casting function as the sensor material. The electrical conductivity of the SWCNT network changes reproducibly upon exposure to various gases and vapours. Selectivity to specific gases, for example, chlorine and hydrochloric acid vapour, is demonstrated by coating the SWCNTs with CSM [36]. Versatility of CSM

rubber in the electrical area is also proved in another experiment. The applicability of polyurethane/CSM rubber blend in such purposes also reported elsewhere [37, 38]. The author developed blends of polyurethane (Vibrathane-SO08 Uniroyal Co., USA) and Hypalon (CSM-350 Du Pont, USA) by three different blending techniques. The ease of processing of the polyurethane rubber was improved as a result of blending with CSM. Experimental data discovered that preheating of the blends, before addition of curatives, enhanced the thermal properties of the blends. The degradation process was delayed along with the retardation in weight loss. The extractability of the single phase by solvent was also restricted on preheating, due to interchain crosslinking reaction. Thus, these typical blends might be used in electrical appliances. Ionic crosslinking efficiency is thoroughly investigated in the presence of silica filler by Owczarek et al. They hypothesized through experimental observation that the CSM rubber composites are formed with core-shell type ZnO-silica engineered particles that paly a novel type crosslinker system [39]. For electrically applicable grades where zinc oxide is enormously used as crosslinker, in this cases zinc oxides not only act as crosslinker but also help to enhance composite strength due to its surprising heat conductivity in the arrested system also [38]. The possible use of zinc oxide and inclinations to substitute CB with precipitated silica modification was achieved to use a new light reinforcing filler with a “core-shell” structure coated with a layer of zinc oxide (ZnO/SiO_2) [39, 40]. CSM is used in rubber engineering due to its prodigious properties resulting from the saturated polymer structure. The vulcanized form of CSM can be used in the production of conveyor belt lining or cable and conductor insulation [41]. Organic acids, thiazoles, dithiocarbamates, or metal oxides are used in CSM crosslinking. The silica containing zinc oxide suggested lower tendency to constitute its own structure in paraffin type oil, which was confirmed by rheological measurements. Zinc oxide doped on the exterior surface of silica particle was a more efficient crosslinking agent as compared to the zinc oxide solely incorporated to the rubber blend in the preparation process. The new filler having a “core-shell”-type architecture enormously amended mechanical properties. The modulus and tensile strength of such vulcanizates were higher in comparison with those with unmodified silica. Silica modified with zinc oxide participated in forming aggregative bonds of the elastomeric network, which was evidenced by high rates of physical relaxation at room temperature. These types of composites revealed the mixture or blend quality as well as their efficiency in the accelerator system. The blend is enriched with well-dispersed silica which can be wholly distributed throughout the rubber matrix [39].

4 Electronic Applications

4.1 Conducting Coating Application

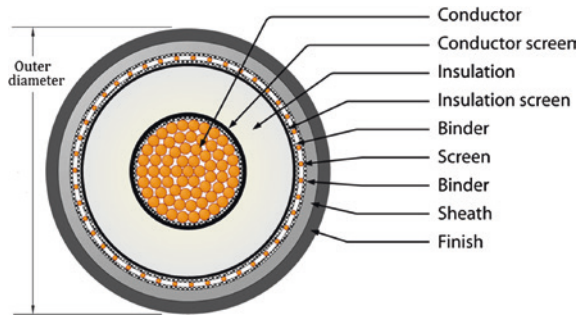
CSM-modified high chlorinated polyethylene (HCPE) anticorrosive coating was canvassed in the paper of Jian, Li et al., and the microstructure and its influence

on properties were investigated by transmission electron microscope (TEM) photographs. Results indicated that HCPE particles were implanted in the dispersed phase of CSM rubber, which can improve flexibility of paint film [40]. Meanwhile, it is good for keeping excellent adhesion and toughness of HCPE with low content of CSM in this coating. Besides, the flexibility of CSM-modified HCPE anti-corrosion paint is superior to other available paints [41]. The coating applications are also widely exploited in acrylic rubber-based coating application which is also reported elsewhere [42]. Conducting coating applications with sensing behaviour are also achieved by CSM rubber-based nanocomposites. Here, CNT-based gas sensor system was developed for discriminating gases and vapours. The sensor array was framed of nanomaterials, e.g., pristine SWCNTs, and SWCNTs with different metal dopants and CSM rubber coatings. This sensor system was exposed to NO₂, HCN, HCl, Cl₂, acetone, and benzene in parts per million (ppm) concentration levels. The arrangement of the developed nanocomposite data was normalized for eradicating concentration and background noise. The postprocessed arrangement data were then subjected to a principal component analysis and a pattern recognition technique for gas and vapour to distinguish [43]. A novel ceramic filler-impregnated CSM-based composite was developed by Oikonomou et al. where a hexagonal ferrite system was synthesized by sol–gel technique. Ba(Co, Zn)₂W-type hexagonal ferrites, prepared by a citrate sol–gel method, have been used as fillers in five layers of CSM composite. Hexagonal ferrites are well long familiar as a class of shielding material with electromagnetic properties (conductivity, permittivity, and permeability) suitable for electromagnetic interference (EMI) prohibition and radar absorbing material (RAM) coatings from centimetre to sub-millimetre wavelengths of the electromagnetic spectrum. Adding an outer layer with carbonyl iron filler, a thin quasi-double-layer microwave absorber has been fabricated that exhibits reflection loss (RL) of 12 dB at 5–12 GHz with a broad minimum of 18 dB at 7.5–9.5 GHz. Layer succession has been optimized for 2 mm total thickness and minimum RL at the X-band as reported by the authors [44].

4.2 Wire and Cable Application

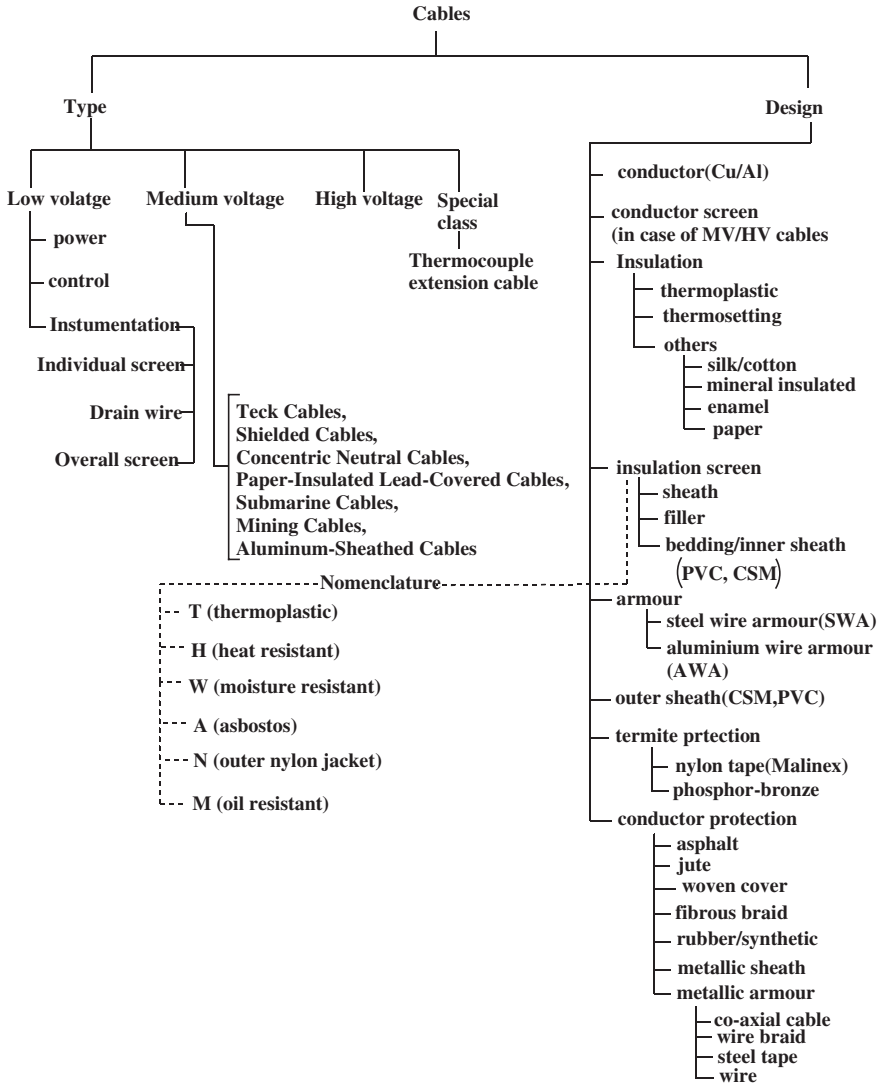
Venturing the discipline of power conveying without power loss is a challenging outcome of several scientific experimentations. Conductor choice depends on ampacity, voltage, mechanical properties, desirable flexibility, enormous dimensional stability, and very acutely cost-effectiveness. The most commonly used metals for conducting core of wire or cables are copper and aluminium possessing solid or stranded winding-type architecture. There are two basic components in a low-voltage cable: the conductor and the electrical insulation (dielectric). There are different types of conductors and insulations. Sometimes, jackets or armouring are added. As voltage increases, other components are added to handle higher electrical stresses. The purpose of this paper is to discuss each component and to

Fig. 6 Typical cable cross section



help an engineer specify the type components required for specific applications. The cable cross-sectional view is elaborated in Fig. 6 as below. It normally consists of two parts with core and outer sheath. Core is the main conductor which carries current, and the outer sheath is the insulation part. Here, the metallic conductor (aluminium, copper) core either in single-core formation or in multicore texture is basically due to the betterment of flexibility. The outer sheath is fabricated by compounded rubber due to their flexibility, weather-resistant nature, insulation behaviour, ease of processing and fabrication, and relatively low cost. The CSM is such a special-purpose one which is normally included in the inner sheath material for its effective adhesion with metal due to its polar moiety (chlorine group) which interacts with the metal as well as outer sheath compound; besides, this CSM rubber is also used in outer sheath also (Scheme 4). The outer sheath should have the effective weather-resistant quality and efficient ultraviolet (UV) resistance. CSM plays an enormous role in such applications due to the absence of unsaturation and chromophore groups (chromophores are liable for UV degradations). The flexibility well balanced with stiffness due to a soft–hard combination of crystalline–amorphous domains inherently present in the CSM rubber makes it an effective outer sheath material.

The atomic energy is most promising for uninterrupted, pollution-free, highly productive source of energy. Countries with forward-thinking atomic/nuclear energy have been investigating methods for assessing the ageing of cables in nuclear power plants (NPPs) and investing on continued research efforts to explore new approaches [45, 46]. Cables used in NPPs must be contrived to last through the plant life on account of the high cost of cable replacement and the complexity of the process. However, cables installed in some speciality areas such as containment buildings may degrade faster than the normal ageing rate, thus impacting cable quality [47, 48]. CSM is synthesized via simultaneous chlorination and chlorosulphonation of polyethylene as feed. Crosslinking can be achieved by using different curing methods (e.g., sulphur, peroxides, and maleimide) to produce commercial generic Hypalon rubber-made cable jackets [49–53]. CSM is a significant and widely used rubber and is mostly used as a sheathing material for electrical cables employed in nuclear power facilities. It is also used in autosupplies, life-saving equipment, and building materials [54, 55]. Jeon, Hwang-Hyun, et al.



Scheme 4 Cable design overview

measured the dielectric properties of CSM rubber-based cable sheath compound where they revealed that in the sea water atmosphere, the water soaked may disturb the inherent electrical properties of a compounded cable sheath material. He studied dielectric constant of CSM decreases marginally as the number of dried days at room temperature increases. Therefore, dielectric constant cannot be used to determine the degree of deterioration of accelerated thermally aged CSM. The insulation property of cables in NPPs is decreased because of sea water flooding,

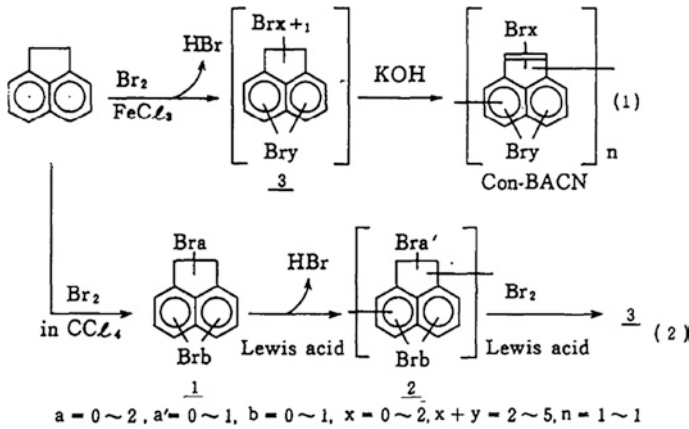
and the insulation property can be retrieved through freshwater flooding. The volume electrical resistivity, peak binding energy, and microstructural analyses of CSM-based materials suggest appraising the possibility of the ageing state of stimulated thermally aged CSM based on the elongation at break (EAB) and apparent density. It is worth mentioning that the volume electrical resistivity of accelerated thermally aged CSM is lower than that of non-accelerated thermally aged CSM, and the insulating property of non-accelerated thermally aged CSM recovers faster than that of accelerated thermally aged CSM [56].

4.2.1 Special-Purpose Flame-Resistant Cable Application

CSM is a special-purpose elastomer on account of its ideal balance of holdings such as ozone, oxygen, weather, heat, oil, and chemicals resistance with good mechanical properties. Due to the presence of the sufficient polarity of the chlorine group in CSM, it is widely used as blends. In this context, NR/CSM blends are commonly practiced blend which customizes properties such as resistance to ozone, oil, heat, flame, and non-polar chemicals. Grounded on chemical structure, the NR/CSM blend may be an issue in materials' inferior mechanical properties because of the incompatibility originating from the mismatch in polarity [57, 58]. This result was the repetition when higher polarity such as fluoro elastomers is blended with NR [59]. The difference in polarity of the rubbers causes high interfacial energy, which is damaging. It will critically limit mixing at the interface and hence the opportunity for crosslinking between the rubbers. It also causes poor phase morphology, which is characterized by large phase sizes. These problems can be mitigated to an extent by the use of suitable modifiers that minimize the phase separation and increase interfacial adhesion; these include the addition of physical or chemical compatibilizers [60, 61]. The self-crosslink reaction between ENR and CSM improves cure time and automotive fuel resistance. ENR could also be used to improve automotive fuel in the blend system. The optimal concentration of ENR is 5 phr. The good mechanical properties as well as automotive fuel resistance were also achieved when ENR > 5 phr [62].

4.2.2 Shielded Electronic Cable Application

At an early stage, Eisuke Oda et al. developed a cable coating formulation where CSM acts as a rubber sheathing material. In that work, condensed bromoacenaphthylene (Con-BACN) was synthesized and later on incorporated into rubber phase due to its extraordinary radiation shielding efficiency as well as flame resistance property. Con-BACN improves the radiation resistance of polymer matrices. The plausible mechanisms were (i) energy channelized from the polymer matrix to Con-BACN molecules; (ii) radical-scavenging graft reactions of Con-BACN to the polymer backbone; and (iii) energy transfer from methylene linkages to aryl



Scheme 5 Synthesis scheme of Con-BACN [63]. Copyright 2012. Reproduced with permission from IEEE

groups of grafted Con-BACN (Scheme 5). The composite showed the radiation resistance of CSM sheet. Con-BACN-bearing sheets show less decrement in elongation accompanying irradiation than do raw sheets; thus, these results indicate that radiation degradation is curbed. The radiation shielding of the cables, with sustained flexibility and the elongation of their insulation and sheath, is excellent at 600 Mrad. The cables can therefore be used not only in the limited wiring of NPPs, but also in any area such as high-level radioactive waste deactivation facilities where flexibility is commanded under exposure to radiation [63].

4.3 CSM Applications in Sensor and Actuator Field

Fabrication of microelectromechanical (MEM) devices in order to apply in the sensor and actuator development is a potential field in recent days. Gas sensors or chemical sensors are attracting magnificent interest on account of their far-flung practical application in industry, environmental supervising, space geographic expedition, medical specialty, and pharmaceuticals. Gas sensors with high sensitivity and selectivity with high confidence levels are demanded for leakage detections of explosive gases viz. hydrogen, and for real-time detections of pathogenic or any sort of lethal gases in industries. There is also a strong demand for the ability to monitor and control our ambient environment, particularly with the raising concern of the globe warming [64]. Typically, there are various introductory criteria for good and efficient gas-sensing systems: (a) high sensitivity and selectivity; (b) fast response time and retrieval time; (c) low functioning temperature and temperature independency; (d) low analyst consumption; and (e) stability in performances. Commonly used gas-sensing materials include vapour-sensitive polymers,

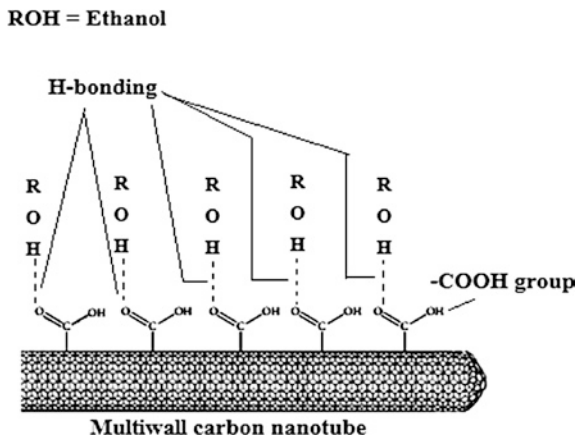
semiconductor metal oxides, and other porous structured materials such as porous silicon [65–67].

Organic synthetic polymers or composites based on elastomers are one of the principal materials implemented in gas-sensing systems. Some conducting polymers can behave like semiconductors due to their transient inherent electron cloud generation compounds which display physicochemical characteristics. As a matter of fact, reversible changes in the detection level's conductivity can be detected upon polar material adsorption on the surfaces at ambient temperature [68]. This outcome is considered to be caused by the charge transfer among gas molecules and the polymer [69]. A typical schematic diagram of the chemically functionalized CNTs is shown in Fig. 7 [70].

The perception features of polymer-coated CNTs in nanocomposite film to particular gases were also investigated. Typically, CNTs do not have sensing response to all gases and vapours but only the ones with high adsorption energy or that can interact with them. The coating or doping of a material on CNTs' surface may diversify the application range. The sensing character of the same structure but with polymer coatings on CNTs can be achieved. The CSM was dissolved in tetrahydrofuran (THF) solvent as a coating solution for Cl_2 sensing, and hydroxypropyl cellulose (HPC) was dissolved in chloroform as coating to detect HCl. The resistance of polymer-coated SWCNT film changed upon exposure to Cl_2 and HCl, while uncoated pure SWCNTs showed no sensing signal. The sensing response demonstrates a huge potential of using modified CNT gas-sensing materials for a broad range of gases and chemical vapours [71].

In sensing applications as artificial muscles, polymers already adopt a wide area of functional advanced materials. Natural muscles have self-repairing potentiality providing billions of work cycles with greater than 20 % of contractions at a speed of 50 % per second, stresses of approximately 0.35 MPa, and adjustable strength and stiffness [72]. Artificial muscles have been attempted for artificial

Fig. 7 Proposed mechanism for alcohol vapour detection using functionalized CNT sensors. The COOH groups tend to form hydrogen bonding with the ethanol molecules at room temperature



hearts, artificial limbs, air vehicles, and humanoid robots. Diverse artificial muscles have been investigated for high response rate, large strain, and eminent output power at minimal strain employing their own material characteristics [73]. Among the family of artificial muscles, the dielectric elastomers have typical lineaments of low specific gravity, flexibility, moderate cost reduction, and easy fabrication, which survives it in many attractive applications such as mobile robots, micro-pumps, microvalves, disc drives, flat panel speakers, and intelligent endoscope. [74–79].

Dielectric elastomer-based actuators have been known for their unique properties of large elongation strain (120–380 %), large stresses (3.2 MPa), high specific elastic energy density (3.4 J/g), high speed of response in 10^{-3} s, and high peak strain rate (34,000 %/s) [79]. Another advantage of dielectric elastomer actuators is the functioning of elastomer actuators can be tailor-made by choosing dissimilar types of elastomers, altering the crosslinking chemistry of polymer chains, adding functional entities, and improving fabrication techniques with ease and versatility in most works. The deformation of elastomers follows with the theories of rubber elasticity and nonlinear viscoelasticity. When an electrical field is applied, the elastomer distortion is tempted primarily by the inherent properties of moduli and dielectric constants of elastomers. Additionally, desirable actuation potentialities are frequently restricted by the dielectric strength (or breakdown voltage) of respective elastomer films. The property processing structure relationship of elastomers particularly below the electrical field and large deformation should be understood on the basis of the fundamental principles of deforming elastomers and practical experience in actuator fabrication. The electrical properties and modulus of the different rubber are shown in Table 3.

Extreme sensitivity to surface adsorption phenomena that make a way for SWCNTs into sensing devices is a very efficient practice. Even so, a practical sensor demands to have selective response in addition to sensitivity. Vichchulada, Pornnipa, et al. have focused on efforts to increase selectivity in SWCNT sensors. This manuscript article presents recent progress towards incorporation of SWCNTs into enhanced sensor and electronic applications. SWCNTs are in nanometre scale with properties that have made them the foci of research for a diversified outcome in electronic applications. In particular, SWCNT gas sensors have experienced significant interest recently. Electrical transducers based on supervising the alteration of conductance or threshold voltage of SWCNT devices upon exposure to an analyte shows the advantage of being simple and low power devices [82].

Solvent-free method to prepare proton-conducting membranes based on commercial elastomers is an effective practice. CSM-based elastomeric blends were studied where the CSM phase used as the matrix materials in the preparation of non-fluorinated proton exchange membranes utilizing a solvent-free route via the in situ reaction of sodium 4-styrenesulphonate (NaSS) as monomer. The morphology of the elastomer/NaSS vulcanizates was deliberated to assess the effect of polarity, viscosity, and saturation degree of the elastomer matrixes. Much better

Table 3 Dielectric and mechanical properties of elastomers

Material	Dielectric constant at 1 kHz	Dielectric loss factor at 1 kHz	Young's modulus ($\times 10^6$ pa)	Engineering stress (MPa)	Break stress (MPa)	Ultimate strain (%)
IR, NR [80]	2.68	0.002–0.04	1.3	15.4	30.7	470
CR [80, 81]	6.5–8.1	0.03/0.86	1.6	20.3	22.9	350
BR [80]	–	–	1.3	8.4	18.6	610
Poly(isobutene-co-isoprene) butyl rubber [80]	2.42	0.0054	1	–	17.23	–
Poly(butadiene-co-isoprene) butyl rubber	5.5 (10^6 Hz)	35 (10^6 Hz)		16.2	22.1	440
Poly(butadiene-co-styrene) (SBR, 25 % styrene content) [80, 81]	2.66	0.00009	1.6	17.9	22.1	440
Poly(isobutyl-co-isoprene) (IIR) [80]	2.1–2.4	0.003	–	5.5	15.7	650
CSM [80]	7–10	0.03–0.07	–	–	24.13	–
EPR [80]	3.17–3.34	0.0066–0.0079	–	–	20.68	–
EPDM [80]	3.0–3.5	0.0004 at 60 Hz	2	7.6	18.1	420
Urethane [80]	5–8	0.015–0.09	–	–	20.55	–
Silicone [81]	3.0–3.5	0.001–0.01	–	–	2–10	80.500

dispersion of NaSS was found in CSM rubber and hydrogenated nitrile butadiene rubber (HNBR) matrixes than in the other three types of elastomer matrixes due to fractional polarity in them which is the main driving force of compatibilization. The CSM/NaSS and HNBR/NaSS proton exchange membrane exhibited the proton conductivity as high as $\sim 0.03 \text{ S cm}^{-1}$, and the ratio of proton conductivity to methanol permeability is achieved higher than that of Nafion [83].

4.3.1 Why Elastomers Deform in the Presence of Electric Stimuli?

The response due to the presence of external electrical stimuli helps the elastomers' deformation to a surprising degree. The physics behind this extraordinary behaviour is hypothesized by R. Pelrine [84]. The concept of electronic behaviours explicitly divulges by the electrostatic energy which is already stored in the elastomer systems with an arbitrary amount of film thickness " z " and surface area " A ". The electrostatically stored energy can be written as in the Eq. 3,

$$U = \frac{Q^2}{2C} = \frac{Q^2 z}{2\epsilon_0 \epsilon_r A} \quad (3)$$

where C , Q , ϵ_0 , and ϵ_r are the capacitance, electrical charge, free-space permittivity (8.85×10^{-12} F/m), and relative permittivity, respectively. The capacitance is defined in Eq. 4,

$$U = \frac{\epsilon_0 \epsilon_r A}{z} \quad (4)$$

From this above equation, the deviation in electrostatic energy can be related to the differential changes in thickness (dt) and area (dA) with a constraint that the total volume is constant ($At = \text{constant}$). Then, the electrostatic pressure generated by the actuator can be derived as below,

$$P = \epsilon_0 \epsilon_r E^2 = \epsilon_0 \epsilon_r (V/z)^2 \quad (5)$$

where E and V are the applied electric field and voltage, respectively.

The electrostatic pressure in previous equation is doubling larger than the pressure in a parallel plate capacitor. This attributes the fact that the energy would switch over with the changes in both the thickness and area of contact of actuator systems.

Actuator performance has been calculated by Eq. 4, and the Hooke's law with Young's modulus (Y) relates the stress (precisely electrostatic pressure) to thickness strain (s_t) as

$$P = -Ys_z \quad (6)$$

where $t = t_0(1 + s_z)$ and t_0 is the initial thickness of the elastomer film. Using the same constraint that the volume of the elastomer is conserved,

$$(1 + S_x)(1 + S_y)(1 + S_z) = 1,$$

$S_x = S_y$ (in-plane strain) can be derived from Eqs. 3 to 4. The through thickness strain S_z can be converted to in-plane strain by solving the quadratic equation for the strain constraint as

$$S_x = (1 + S_z)^{-0.5} - 1. \quad (7)$$

For low-strain materials, the elastic strain energy density (U_e) of actuator materials has been estimated which also shows proportionality to Young's modulus of the material [84]

$$U_e = \frac{1}{2}PS_z = \frac{1}{2}YS_z^2 \quad (8)$$

In general, for high-strain materials, the in-plane expansion upon the compression phenomena markedly envisioned as the material is compressed, and therefore, the elastic U_e can be obtained by integrating the compressive stress times the varying planar area over the displacement, ensuing in the adopting Eq. 9 [84]

$$U_e = \frac{1}{2} P \ln(1 + S_z) \quad (9)$$

4.4 CSM-Based Radiation Shielding Applications

4.4.1 Mechanisms of Electromagnetic Interference (EMI) Shielding

EMI shielding pertains to the reflection and/or adsorption of electromagnetic radiation by means of a material which plays a role in shielding with proficiency against the incursion of the radiation through the shield. Electromagnetic radiation, especially at high frequencies (i.e. radio waves, radiation emanating from cellular phones), tends to interfere with electronics. EMI shielding of electronics as well as radiation source is vehemently required also by the governments around the world. EMI shielding is a slight bit distinguished from the magnetic shielding. The mechanisms of radiation shielding are lucidly stated which were resulted from several hypotheses.

Basically, two major mechanisms are reflected in papers: one is primary mechanism and another one is secondary mechanism. It is also noteworthy that the primary one is related to the reflection phenomena and the latest one is the absorption.

Primary Mechanism of Shielding: Reflection

In case of primary mechanisms, the utmost priority to be a shielding prohibition is that material should be a mobile charge carrier that may come from either electrons or mobile hole carriers. These conducting particulate matters interact with the electromagnetic waves; hence, it is proved that conductivity is prime here but not necessarily very high conductivity. Electrical conductivity is not the essential scientific prerequisite item for shielding. Shielding does not require connectivity, and it is enhanced by connectivity [85]. Metals are the most common materials for EMI shielding. These EMI shielding is mainly by reflection due to the inherent free electrons cloud. But metal sheets are bulky, so metal coatings, made by either electroplating, electrodeless plating or vacuum deposition are used for radiation shielding [86–88].

Secondary Mechanism of Shielding: Absorption

A secondary mechanism of EMI shielding is usually absorption. Significant absorption of the radiation by the shield is due to the electric and/or magnetic dipoles intrinsically occurred in the shielding materials, which interact with the electromagnetic fields exposed to the radiation. The electric dipoles generally provided by BaTiO₃ or other materials having sufficiently high value of the dielectric

Table 4 Electrical conductivity relative to copper (σ_r) and relative magnetic permeability (μ_r) of selected materials [92]

Material	σ_r	μ_r	$\sigma_r\mu_r$	σ_r/μ_r
Silver	1.05	1	1.05	1.05
Copper	1	1	1	1
Gold	0.7	1	0.7	0.7
Brass	0.61	1	0.61	0.61
Bronze	0.18	1	0.18	0.18
Tin	0.15	1	0.15	0.15
Lead	0.08	1	0.08	0.08
Nickel	0.2	100	20	2×10^{-3}
Stainless steel (430)	0.02	500	10	4×10^{-5}
Mu-metal (at 1 kHz)	0.03	20,000	600	1.5×10^{-6}
Superpermalloy (at 1 kHz)	0.03	100,000	3000	3×10^{-7}

constant. The magnetic dipoles may be provided by some sort of magnetic particles viz. Fe_3O_4 or other magnetic materials having a prominent value of the magnetic permeability [86], which may be enhanced by reducing the number of magnetic domain walls through the use of a multilayer magnetic films [89, 90].

The absorption loss is designated by $\sigma_r\mu_r$, whereas the RL is a function of the ratio σ_r/μ_r , where σ_r is the electrical conductivity relative to copper and μ_r is the relative magnetic permeability. Table 4 shows these factors for various materials. Silver, copper, gold, and aluminium are splendid for reflection, due to their high conductivity. Superpermalloy and Mu-metal are excellent for absorption due to bearing of their high magnetic permeability. The RL recedes with evoking frequency, whereas the absorption loss increment is directly related to frequency.

The absorption loss represents the “skin effect” attenuation among the thickness of the material, and it is the function of its relative permeability and conductivity. The attenuation through absorption via a shield of thickness “ t ” is given by the Eq. 10 [91]

$$A(\text{dB}) = 131.4t\sqrt{f\mu_r\sigma_r}. \quad (10)$$

Theory of Multiple Reflections

In addition to reflection and absorption, a multiple reflection, which is basically the consecutive reflections at respective surfaces or interfaces in the shield, is also contributing to shielding. This mechanism needs the presence of a more surface area or interface area in the shield. Any porous substrate or foam-type materials are the relevant examples with large surface area, and conducting particulate materials are also the examples with sufficient surface area in composite-type materials. The loss due to multiple reflections in the respective shields can be neglected when the skin depth is lower than the distance between the reflecting surfaces and interface. The

losses, which may be either due to reflection or absorption or multiple reflections, are usually expressed in dB; hence, the algebraic sum of all the losses is the shielding effectiveness (SE, expressed in dB). The absorption loss is directly proportional to the thickness of the shielding material or composite. Electromagnetic radiation at high frequencies pervades exclusively the near surface region of an electrical conductor. This is known as the skin effect. The electric field due to a plane wave penetrating a conductor drops exponentially with enhancement of depth into the conductor. The depth at which the field drops to $1/e$ of the incident value is anticipated as the skin depth (δ), which is expressed in Eq. 11

$$\delta = \frac{1}{\sqrt{\pi f \mu \sigma}} \quad (11)$$

where f = frequency, μ = magnetic permeability = $\mu_0 \mu_r$, μ_r = relative magnetic permeability, $\mu_0 = 4\pi \times 10^{-7}$ H/m, and σ = electrical conductivity in $\Omega^{-1}\text{m}^{-1}$.

The losses by multiples reflection are given by Eq. 12 [91]

$$M(\text{dB}) = 20 \log\left(1 - e^{-2\frac{t}{\delta}}\right) \quad (12)$$

Multiple reflections and transmissions can broadly dismiss for shield thicknesses which are practically greater than a skin depth. The coefficient is negative; the multiple reflections reinforce the field transmitted to the output of shielding. At low thickness of the material with respect to the thickness of skin, it is accepted that multiple reflections take place on the interface. When the thickness of the material is the identical magnitude with the thickness of skin, reducing electromagnetic fields is less. The term “ M ” multiple reflections is negligible.

4.4.2 Chlorosulphonated Polyethylene Used in Radiation Shielding Applications

Electrically conductive polymer composites have invoked a great deal of scientific and commercial concern. The possible mechanistic pathway of electrical conduction in these composites is the organization of a continuous network of conductive fillers throughout the insulating polymer matrix. Conductive composites have been widely applied in the area of electromagnetic/radio-frequency interference (EMI/RFI) shielding, electrostatic discharge (ESD), conductive adhesives for die attach in electronic packaging applications, and elastomer interconnect devices used for integrated circuit (IC) package fabrication [93]. Electrically conductive elastomer composites, which display variable conductivity in response to varying external loading, are widely used for various electronic applications, such as touch-control switches and strain and pressure sensors for applications in robot hands or artificial limbs, gaskets etc. As per ASTM designation, the working formula for SE is

$$SE = 10 \log \frac{P_1}{P_2} \quad (13)$$

where P_1 is the obtained power with the material present and P_2 is the obtained power without the material present.

EMI shielding is the consequence of reflection (R), absorption (A), and internal multiple reflection (I) of the incident electromagnetic waves in the samples. These three quantities are related to each other by the following expression for SE:

$$SE = 10 \log \frac{P_1}{P_2} = (R + A + I) \quad (14)$$

“ I ” is negligible when A is over 10 dB or greater than 15 dB. R and A are given by the following equation [94, 95]

$$R = 108 + \log \frac{G}{\mu f} \quad (15)$$

$$A = 1.32t \sqrt{G\mu f} \quad (16)$$

where G is the conductivity of the samples relative to copper, m is the magnetic permeability of the sample relative to vacuum or copper (m is usually 1.0), f is the radiation frequency in MHz, and t is the thickness of the specimen in cm. Here, a microwave absorbing rubber composites was prepared by addition of conductive CB and aluminium powder in NR, ENR, and CSM where the comparative study followed by the selection of rubber system to enhance the SE was investigated. The range of frequencies (8.5–12 GHz) and the effect of fillers on SE of three rubber systems were similar. SE of the rubber increased from lower level (i.e. <1 dB) to 18–28 dB for 50 phr loading of CB or to 30–40 dB for 50 phr loading of CB and 50 phr of aluminium powder. While the conductivity was higher, aluminium powder was less effective than conductive CB because of the lower volume fraction and larger grain size, hence lesser dispersion in the rubber matrix. It is hereby significant that the impregnation of binary filler exhibited higher SE than single filler. SE of the rubber composites can be ranked in the following order, ENR > CSM > NR, and a rank of their mechanical properties, excluded compression set, was CSM > ENR > NR. The SE (dB) is plotted with frequency (Hz) as shown in Fig. 8.

PANI-impregnated CSM is another fruitful development of radiation protective film. PANI and its derivatives or modified PANI have generated enormous involvement among scientists and technologists because of their wide variety of desirable properties and potential technological applications. Outcome of secondary doping of PANI composites, synthesized by in situ emulsion polymerization of aniline in the presence of CSM or SBS and dodecyl benzene sulphuric acid (DBSA) on conductivity, was investigated [97]. PANI can be doped by perchloric acid or an organic sulphonic acid (camphor sulphonic acid, CSA), and the dielectric behaviours are studied. CSA doped samples evidenced better properties which can be used as efficient filler for the development of inorganic–organic hybrid shielding materials which also reported elsewhere [98].

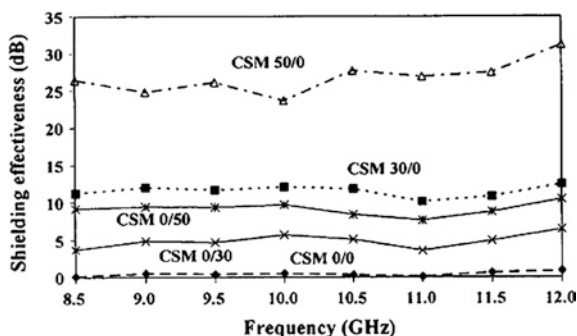


Fig. 8 Effect of filler in CSM matrix to measure SE [96]. Copyright 2007. Reproduced with the permission from John Wiley & Sons

5 Conclusion

The quite promising applicability of chlorosulphonated polyethylene in the electronic application area is a well-practiced topic now in rubber commercialization. The eminent compatibility with the conducting organic as well as inorganic particulate materials can sharpen the exploitation of CSM conducting composites for electronic applications. The flexibility as well as weather resistance makes this material more applicable in external service use. The manufacturing procedures of CSM are elucidated also where the solution-suspension method and the gas phase methods are emphatically explained due to their acceptability for green and better yield. Altering the feed quality from crystalline to amorphous arrangements, the increment of yield and ease of synthesis are also documented. The electronic behaviours such as fabricated flexible electronic devices, MEM, sensors and actuators, and shielding materials where they are loaded with conducting particulate materials are authenticated from the several scientific publications as already documented in this chapter. The wide range of applications are not only in the electronic fields such as electronic coating and cable jacketing either as sheath or inner core material formulations but also in the efficient EMI/RFI/radiation shielding material fabrication and conduction adhesive applications. Sensor and actuator fields make this material with high proficiency in end use. The actuation behaviours are well established by the mathematical models of various scientists, and the deformation functions with the electrical pulse are also studied here. Besides these works, there are wide scopes for graphene oxide-impregnated CSM which is now not practiced enormously for achieving better conducting, flexible, high strength rubber composite comparatively to other commercial rubber composite for radiation shielding applications. The in situ reduction to prepare graphene from the graphene oxide is also an upcoming field to cultivate the radiation pollution inhibition as well as flexible electrosensors and actuators.

References

1. Schweitzer PA (ed) (2004) Encyclopedia of corrosion technology (vol 20, p 138). CRC Press, New York
2. Morrell SH (1982) Rubber technology and manufacture. Blow, CM, Ed 162, p 135
3. Tanrattanakul V, Petchkaew A (2006) Mechanical properties and blend compatibility of natural rubber–chlorosulfonated polyethylene blends. *J Appl Polym Sci* 99(1):127–140
4. Chowdhury S, Das CK (2000) Structure–shrinkability correlation in polymer blends of ethylene vinyl acetate and chlorosulfonated polyethylene. *J Appl Polym Sci* 78(4):707–715
5. Antony P, Datta S, Bhattacharya A, De SK (2001) Mixed crosslinking in chlorosulfonated polyethylene and its blend with ethylene vinyl acetate copolymer. *J Elastomer Plastics* 33(3):196–210
6. Chowdhury S, Das CK (2001) Development of heat shrinkable and flame-retardant EVA/CSM blends. *Fire Mater* 25(5):199–202
7. Gupta S, Chowdhury SR, Mishra JK, Das CK, Patra PK, Tripathy AK, Banerjee MS (2000) Heat-shrinkable polymer blends through interchain crosslinking based on ethylene propylene and chlorosulfonated polyethylene. *Mater Lett* 46(2):125–130
8. Calmet JF, Carlin F, Nguyen TM, Bousquet S, Quinot P (2002) Irradiation ageing of CSPE/EPR control command electric cables. Correlation between mechanical properties and oxidation. *Rad Phys Chem* 63(3):235–239
9. Giurginca M, Zaharescu T (2000) Thermal and radiation behaviour of HNBR and CSPE blends. *Polymer* 41(20):7583–7587
10. Roychoudhury A, De PP (1997) Studies on chemical interactions between chlorosulphonated polyethylene and carboxylated nitrile rubber. *J Appl Polym Sci* 63(13):1761–1768
11. Mukhopadhyay S, De PP, De SK (1991) A self-vulcanizable and miscible blend system based on hypalon and carboxylated nitrile rubber. *J Appl Polym Sci* 43(2):347–355
12. Roychoudhury A, De PP, Bhowmick AK, De SK (1992) Self-crosslinkable ternary blend of chlorosulphonated polyethylene, epoxidized natural rubber and carboxylated nitrile rubber. *Polymer* 33(22):4737–4740
13. Antony P, De SK, van Duin M (2001) Self-crosslinking rubber/rubber and rubber/thermoplastic blends: a review. *Rubber Chem Technol* 74(3):376–408
14. Roychoudhury A, De PP (1997) Studies on chemical interactions between chlorosulphonated polyethylene and carboxylated nitrile rubber. *J Appl Polym Sci* 63(13):1761–1768
15. Mukhopadhyay S, Chaki TK, De SK (1990) Self-vulcanizable rubber blend system based on epoxidized natural rubber and hypalon. *J Polym Sci Part C Polym Lett* 28(1):25–30
16. Roychoudhury A, De PP, Dutta NK, Roychoudhury N, Haidar B, Vidal A (1993) FTIR and NMR studies on crosslinking reaction between chlorosulfonated polyethylene and epoxidized natural rubber. *Rubber Chem Technol* 66(2):230–241
17. Wang Z, Ni H, Bian Y, Zhang M, Zhang H (2010) The preparation and thermodynamic behaviors of chlorosulfonated polyethylene. *J Appl Polym Sci* 116(4):2095–2100
18. Noeske H, Roelen O (1959) U.S. Patent 2,889,259 (CA: 54, 14790c)
19. Zhao R, Cheng S, Shun Y, Huang Y (2001) Preparation of chlorosulfonated polyethylene by the gas-solid method. *J Appl Polym Sci* 81(14):3582–3588
20. Benedirt GM, Hodge IM (1985) E.P. 133,686 (CA: 102, 168178n)
21. Benedirt GM (1984) U.S. Patent 4,452,953 (CA: 101, 39028u)
22. Blanchard RR (1986) U.S. Patent 4,584,351 (CA: 105, 7765y)
23. Bazuin CG, Eisenberg A (1981) Modification of polymer properties through ion incorporation. *Ind Eng Chem Prod Res Develop* 20(2):271–286
24. Xie HQ, Chen Y, Guan JG, Xie D (2006) Novel method for preparation of quaternary ammonium ionomer from epoxidized styrene–butadiene–styrene triblock copolymer and its use as compatibilizer for blending of styrene–butadiene–styrene and chlorosulfonated polyethylene. *J Appl Polym Sci* 99(4):1975–1980

25. Boonsong K, Seadan M, Lopattananon N (2008) Compatibilization of natural rubber (NR) and chlorosulfonated polyethylene (CSM) blends with zinc salts of sulfonated natural rubber. *Songklanakarin J Sci Technol* 30(4):491
26. Nanda M, Tripathy DK (2010) Relaxation behavior of conductive carbon black reinforced chlorosulfonated polyethylene composites. *J Appl Polym Sci* 116(5):2758–2767
27. Mahapatra SP, Tripathy DK, Lee Y (2012) Electrical response of microcellular EPDM rubber composites: complex dielectric modulus formalism and current–voltage characteristics. *Polym Bull* 68(7):1965–1976
28. Brug GJ, Van Den Eeden ALG, Sluyters-Rehbach M, Sluyters JH (1984) The analysis of electrode impedances complicated by the presence of a constant phase element. *J Electroanal Chem Interfac Electrochem* 176(1):275–295
29. Tan Y, Tang J, Deng A, Wu Q, Zhang T, Li H (2013) Magnetic properties and microwave absorption properties of chlorosulfonated polyethylene matrices containing graphite and carbonyl-iron powder. *J Mag Magn Mater* 326:41–44
30. Markovic G, Veljkovic O, Radovanovic B, Marinovic-Cincovic M, Budinski-Simendic J, Sad N (2008) High energy radiation resistance of composites based on NR/CSM rubber blend: influence of carbon black and wood flour. *KGK Kautsch, Gummi, Kunstst* 61(7–8):363–367
31. Marković G, Marinović-Cincović MS, Jovanović V, Samaržija-Jovanović S, Budinski-Simendić J (2012) Gamma irradiation aging of NBR/CSM rubber nanocomposites. *Comp Part B Eng* 43(2):609–615
32. Feng Z, Nuli Y, Yang J (2007) Conductive sulfur-containing material/polyaniline composite for cathode material of rechargeable magnesium batteries. *Acta Phys Chim Sin* 23(3):327–331
33. Meyyappan M (2004) Carbon nanotubes: science and applications. CRC, Boca Raton, FL
34. Moisan M, Barbeau J, Crevier MC, Pelletier J, Philip N, Saoudi B (2002) Plasma sterilization: methods and mechanisms. *Pure Appl Chem* 74(3):349–358
35. Li J, Lu Y, Meyyappan M (2006) Nano chemical sensors with polymer-coated carbon nanotubes. *Sensors J IEEE* 6(5):1047–1051
36. Khatua BB, Das CK, Patra PK, Banerjee MS, Millins W (2000) Speciality polymer blends of polyurethane and chlorosulfonated polyethylene (S-cure). *Int J Polym Mater* 46(1–2):347–360
37. Dick JS (2014) How to improve rubber compounds: 1800 experimental ideas for problem solving. Carl Hanser Verlag GmbH Co KG, München
38. Cannas C, Mainas M, Musinu A, Piccaluga G (2003) ZnO/SiO₂ nanocomposites obtained by impregnation of mesoporous silica. *Comp Sci Technol* 63(8):1187–1191
39. Owczarek M, Zaborski M, Stefanowskiego K (2004) Chlorosulfonated polyethylene elastomers containing zinc oxide incorporated on SiO₂. *Kautsch Gummi Kunstst* 57(5):218–223
40. Jian L, Jun W, Shujun C (1997) Application of chlorosulfonated polyethylene elastomer in coating industry. *Paint Coat ind* 3:016
41. Ding Y, Qiao H, Zhou M (2002) Study on chlorosulphonated polyethylene (CSM) modified high chlorinated polyethylene (HCPE) anticorrosive coatings. *J Chinese Soc Corr Protect* 22(4):221–224
42. Lin TIAN (2006) Status and progress on special synthetic rubber in China. *China Elastomerics* 3:018
43. Lu Y, Partridge C, Meyyappan M, Li J (2006) A carbon nanotube sensor array for sensitive gas discrimination using principal component analysis. *J Electroanal Chem* 593(1):105–110
44. Oikonomou A, Giannakopoulou T, Litsardakis G (2007) Design, fabrication and characterization of hexagonal ferrite multi-layer microwave absorber. *J Magn Mag Mater* 316(2):e827–e830
45. U.S. Nuclear Regulatory Commission/Regulatory Guide 1.218 (2012) Condition monitoring techniques for electric cables used in nuclear power plants. Office of Nuclear Regulatory Research, Apr 2012

46. Gillen KT, Assink R, Bernstein R, Celina M (2006) Condition monitoring methods applied to degradation of chlorosulfonated polyethylene cable jacketing materials. *Polym Degrad Stab* 91(6):1273–1288
47. Assink RA, Gillen KT, Bernstein R, Celina MC (2005) Condition monitoring methods applied to degradation of chlorosulfonated polyethylene cable jacketing materials (No. SAND2005-3251J). Sandia National Laboratories
48. Kim IY, Goo CS, Lee JH, Jin BS, Kang MK, Shin YD (2012) A study of validation of condition monitoring method of NPPs cable through volume electrical resistivity. In International conference on high voltage engineering and application (ICHVE), 2012 (pp 68–71). IEEE
49. Kim KY, Nho YC, Jung SH, Park EH (1999) Development of evaluation technique on ageing degradation of organic polymer in nuclear power plant. Korea Atomic Energy Research Institute, Republic of Korea
50. Li W, Dichiara A, Zha J, Su Z, Bai J (2014) On improvement of mechanical and thermo-mechanical properties of glass fabric/epoxy composites by incorporating CNT–Al₂O₃ hybrids. *Compos Sci Technol* 103:36–43
51. Lee JH, Kang MK, Jeon JS, Lee SH, Kim IY, Park HS, Shin YD (2014) A study on the properties of CSPE according to accelerated thermal aging years. *J Electr Eng Technol* 9(2):643–648
52. Jeon HH, Lee JU, Jeon JS, Lee SH, Shin YD, Effects of dried days on properties of seawater and freshwater flooded CSPE in NPPs
53. Gu Z, Song G, Liu W, Gao J, Dou W, Lu P (2010) Preparation and properties of chlorosulfonated polyethylene/organomontmorillonite nanocomposites. *J Appl Polym Sci* 115(6):3365–3368
54. Chung SK, Lee DC (1996) High voltage engineering. Munundang
55. Gillen KT, Assink RA, Bernstein R (2004) Condition monitoring approaches applied to a polychloroprene cable jacketing material. *Polym Degrad Stab* 84(3):419–431
56. Jeon HH, Lee JU, Jeon JS, Lee SH, Shin YD, Effects of dried days on properties of seawater and freshwater flooded CSPE in NPPs
57. Tanrattanakul V, Petchkaew A (2006) Mechanical properties and blend compatibility of natural rubber–chlorosulfonated polyethylene blends. *J Appl Polym Sci* 99(1):127–140
58. Marković G, Radovanović BC, Budinski-Simendić JK, Marinović-Cincović MT (2005) Curing characteristics of chlorosulphonated polyethylene and natural rubber blends. *J Serb Chem Soc* 70(5):695–703
59. Phiriyawirut M, Luamlam S (2013) Influence of poly (vinyl chloride) on natural rubber/chlorosulfonated polyethylene blends. *Open J Org Polym Mater*
60. Plochocki AP, Dagli SS, Andrews RD (1990) The interface in binary mixtures of polymers containing a corresponding block copolymer: effects of industrial mixing processes and of coalescence. *Polym Eng Sci* 30(12):741–752
61. Sirisinha C, Saeoui P, Guaysomboon J (2004) Oil and thermal aging resistance in compatibilized and thermally stabilized chlorinated polyethylene/natural rubber blends. *Polymer* 45(14):4909–4916
62. Phiriyawirut M, Luamlam S (2013) Improved automotive fuel resistance of natural rubber/chlorosulfonated polyethylene blends by blending epoxidized natural polymer. *Open J Org Polym Mater*
63. Oda E, Fujimura S, Kubo M, Tsutsumi Y, Seguchi T, Hagiwara M (2012) Development of super-radiation-resistant cable. *Int J Radiat Appl Instrument Part C Radiat Phys Chem* 22(3):4003304
64. Ren Z, Lan Y, Wang Y (2013) Carbon nanotubes. Aligned carbon nanotubes. Springer, Berlin Heidelberg, pp 7–43
65. Rittersma ZM (2002) Recent achievements in miniaturised humidity sensors—a review of transduction techniques. *Sens Actuat A Phys* 96(2):196–210
66. Fenner R, Zdankiewicz E (2001) Micromachined water vapor sensors: a review of sensing technologies. *Sensors J IEEE* 1(4):309–317

67. Traversa E (1995) Ceramic sensors for humidity detection: the state-of-the-art and future developments. *Sens Actuat B Chem* 23(2):135–156
68. Bartlett PN, Archer PB, Ling-Chung SK (1989) Conducting polymer gas sensors part I: fabrication and characterization. *Sens Actuat* 19(2):125–140
69. Petty MC, Casalini R (2001) Gas sensing for the 21st century: the case for organic thin films. *Eng Sci Educ J* 10(3):99–105
70. Sin ML, Chun Tak Chow G, Wong GM, Li W, Leong P, Wong KW (2007) Ultralow-power alcohol vapor sensors using chemically functionalized multiwalled carbon nanotubes. *Nanotechnol IEEE Trans* 6(5):571–577
71. Philip B, Abraham JK, Chandrasekhar A, Varadan VK (2003) Carbon nanotube/PMMA composite thin films for gas-sensing applications. *Smart Mater Struct* 12(6):935
72. Ebron VH, Yang Z, Seyer DJ, Kozlov ME, Oh J, Xie H, Baughman RH (2006) Fuel-powered artificial muscles. *Science* 311(5767):1580–1583
73. Bar-Cohen Y (2002) Electro-active polymers: current capabilities and challenges. In: *Proceedings of SPIE, the international society for optical engineering proceedings of SPIE, the international society for optical engineering*, vol 4695, pp 1–7
74. Banerjee S, Banerjee S, Tyagi AK (eds) (2012) *Functional materials: preparation, processing and applications*. Elsevier
75. Pelrine R, Kornbluh R, Pei Q, Joseph J (2000) High-speed electrically actuated elastomers with strain greater than 100 %. *Science* 287(5454):836–839
76. Yang G, Ren W, Akhras G, Mukherjee B (2006) Transverse strain of silicone dielectric elastomer actuators. *J Adv Sci* 18(1/2):166–169
77. Choi HR, Jung KM, Koo JC, Nam JD, Lee YK, Cho MS (2005) Electrostatically driven soft polymer actuator based on dielectric elastomer. *Key Eng Mater* 297:622–627
78. Koo JC, Choi HR, Jung MY, Jung KM, Nam JD, Lee YK (2005) Design and control of three-DOF dielectric polymer actuator. *Key Eng Mater* 297:665–670
79. Shoa T, Madden JD, Fok CWE, Mirfakhrai T (2009) Rate limits in conducting polymers. *Adv Sci Technol* 61:26–33
80. Birley AW (1992) *Physics of plastics: processing, properties and materials engineering*. Hanser Verlag, Munich
81. Lee MJ, Lee NY, Lim JR, Kim JB, Kim M, Baik HK, Kim YS (2006) Antiadhesion surface treatments of molds for high-resolution unconventional lithography. *Adv Mater* 18(23):3115–3119
82. Vichchulada P, Lipscomb LD, Zhang Q, Lay MD (2009) Incorporation of single-walled carbon nanotubes into functional sensor applications. *J Nanosci Nanotechnol* 9(4):2189–2200
83. He S, Lin Y, Wei Z, Zhang L, Lin J, Nazarenko S (2015) Solvent-free fabrication of proton-conducting membranes based on commercial elastomers. *Polym Adv Technol* 26(4):300–307
84. Pelrine R, Kornbluh RD, Eckerle J, Jeuck P, Oh S, Pei Q, Stanford S (2001). Dielectric elastomers: generator mode fundamentals and applications. In: *SPIE's 8th annual international symposium on smart structures and materials, international society for optics and photonics*, pp 148–156
85. Chung DDL (2001) Electromagnetic interference shielding effectiveness of carbon materials. *Carbon* 39(2):279–285
86. Sadchikov VV, Prudnikova ZN (1997) Amorphous materials in electromagnetic shields. *Steel in Transl* 27(4):71–75
87. Shinagawa S, Kumagai Y, Urabe K (1999) Conductive papers containing metallized polyester fibers for electromagnetic interference shielding. *J Porous Mater* 6(3):185–190
88. Kumar R, Kumar A, Kumar D (1997) RFI/EMI/microwave shielding behaviour of metallized fabric—a theoretical approach. In: *Proceedings of the international conference on IEEE, electromagnetic interference and compatibility'97*, pp 447–450
89. Grimes CA (1994) EMI shielding characteristics of permalloy multilayer thin films. In: *Aerospace applications conference proceedings IEEE*, pp 211–221

90. Biter WJ, Jamnicky PJ, Coburn W (1994) Shielding improvement by use of thin multilayer films. In: International sampe electronics conference society for the advancement of material and process engineering, vol 7, p 234
91. Klinkenbusch L (2005) On the shielding effectiveness of enclosures. *Electromagn Compat IEEE Trans* 47(3):589–601
92. Paul CR (1992) Introduction to electromagnetic compatibility. NASA STI/Recon Technical Report A, vol 93, p 49330
93. Taya M, Kim WJ, Ono K (1998) Piezoresistivity of a short fiber/elastomer matrix composite. *Mech Mater* 28(1):53–59
94. Chen G, Zhao W (2010) Polymer/graphite nanocomposites. CRC Press, New York 79
95. Das NC, Khastgir D, Chaki TK, Chakraborty A (2000) Electromagnetic interference shielding effectiveness of carbon black and carbon fibre filled EVA and NR based composites. *Compos A Appl Sci Manuf* 31(10):1069–1081
96. Tanrattanakul V, Bunchuay A (2007) Microwave absorbing rubber composites containing carbon black and aluminum powder. *J Appl Polym Sci* 105(4):2036–2045
97. Xie HQ, Ma YM, Guo JS (2001) Secondary doping phenomena of two conductive polyaniline composites. *Synt Met* 123(1):47–52
98. Thomas RM, John H, Mathew KT, Joseph R, George KE (2009) Optimization of preparation conditions on the dielectric properties of polyaniline. *J Appl Polym Sci* 112(5):2676–2682